Calorimetry for the NLC Detector*

James E. Brau, Anatoli A. Arodzero, and David M. Strom
Physics Department, University of Oregon, Eugene, OR 97403, USA
representing
the NLC Detector Group

ABSTRACT

The physics goals of discovery and measurement at the NLC depend on excellent calorimetry. Of the options, we find a high granularity silicon-tungsten sampling electromagnetic calorimeter combined with a relatively well segmented hadron calorimeter to surpass the requirements. This technique provides enormous strength in understanding the details of jet energy deposition, and therefore, can provide excellent jet energy resolution. We present some ideas of how such a device could be configured and what performance might be expected.

I. INTRODUCTION

Most physics goals of the NLC depend on the performance of the NLC calorimetry. The intermediate mass Higgs search and studies require optimal jet resolutions for Z^0 and Higgs reconstruction[2] , hermiticity for tagging the $Z \to \nu\nu$ mode[2], and good electromagnetic energy resolution for measurement of the $h \to \gamma\gamma$ branching fraction[3]. Suppression of backgrounds to the $e^+e^- \to Zh$ requires good W and Z mass resolution to reject the ZZ and WW production. A 4% unconstrained resolution for Ws and Zs, improving to 2% with the Z h constraint, would be the goal. Top studies will demand precision energy measurements which have implications on calorimetry calibration and resolution. The SUSY searches demand the best possible hermeticity. Elimination of two-photon processes within a bunch train requires timing resolution as near the inter-bunch spacing ($\sim$ 1.4 nsec) as possible.

At higher energies, the study of strongly interacting gauge bosons through $e^+e^- \to \nu\overline{\nu}W^+W^-$ and $\nu\overline{\nu}ZZ$ requires two-jet mass resolution sufficient to distinguish $e^+e^- \to \nu\overline{\nu}W^+W^-$ from $e^+e^- \to \nu\nu ZZ$[1].

The NLC Detector design employs a 4 Tesla solenoidal field, driven by the requirement to protect the vertex detector from the enormous number of e^+e^- pairs produced in the beam-beam interaction[4]. Optimal electromagnetic energy resolution demands that the solenoid be outside the EM calorimeter, and the coil radius should be minimized to contain costs. For this study, a 50 centimeter radius EM calorimeter has been chosen, although larger radii may be required for acceptable separation of electromagnetic showers from charged tracks.

The requirement of optimal EM resolution clashes with optimal jet resolution. Compensated calorimeters, which yield the best jet resolutions, call for compromised EM resolution to provide uniformity between the EM and hadronic sections. The calorimeter-dominated jet measurement technique also relies on a limited disruption of the jet by a modest magnetic field. Our plan for a 4 Tesla field and an EM calorimeter optimized for EM calorimetry runs counter to this approach. We are therefore adopting the strategy of a combined tracker with calorimeter energy measurements. Jets will be measured by using the excellent measurements of the inner tracker for charged tracks, with electromagnetic showers measured in the EM calorimeter, and neutral hadrons detected and measured in the EM or hadronic calorimeter. It is important to note that the NLC inner tracker not only provides much better energy measurements of the charged tracks than the calorimeter could, but does so with nearly 100 percent efficiency, an important requirement for reliable jet energy measurements. The EM calorimeter must be able to provide the best possible separation of EM showers from the charged particles, meaning it must be dense with a small Moliere radius and highly segmented.

The concept of study then is an inner electromagnetic calorimeter, separated in the barrel from the hadronic calorimeter by the solenoidal magnetic coil. The hadronic calorimeter is assumed to be a modest sampling calorimeter but with very good granularity, such as lead/scintillator or steel/scintillator. The bulk of the jet energy is measured in the tracker and the EM calorimeter, and the hadron calorimeter must be very efficient in measuring neutral hadrons. Table I presents the major design goals for the calorimeter.

The main focus of this paper is the electromagnetic calorimeter. The most stringent energy resolution issue for the EM calorimeter is the suppression of the background to Higgs $\to \gamma\gamma$, primarily from $e^+e^- \to \gamma\gamma Z$. The issues for Higgs $\to \gamma\gamma$ are different for an NLC Detector and an LHC Detector. In the latter case this decay mode must provide the discovery, while at the NLC discovery will come easily with the prominent decay modes, and one is measuring the branching ratio of an established state, a qualitatively different task. Figure 1 presents the expected dependence of the fractional error in $\sigma(Zh_{SM}) \cdot BR(h_{SM} \to \gamma\gamma)$ on the EM calorimeter energy resolution[3]. The calorimeters studied and presented in this figure are (I) $2\% \oplus 0.5\% \oplus 0.2\%/E$, (II) $5\%/\sqrt{E} \oplus 0.5\%$, (III) $10\%/\sqrt{E} \oplus 1\%$, and (IV) $12\%/\sqrt{E} \oplus 0.5\%$[3]. Some improvement on these numbers might result from constrained fits to the events. An integrated luminosity of 150 fb^{-1} (three years of design luminosity) is assumed. Clearly there is an advantage to the best possible EM energy resolution. However, this advantage must be evaluated in the context of the trade-offs with losses to other physics goals. The approach taken here is to optimize the overall EM calorimeter performance, which includes resolution, but also other properties such as granularity needed for optimal jet resolution.

A number of options for the EM calorimeter have been considered. As described above we are searching for a technique which will give good energy resolution, with fast (few nanosecond) response, operating in a 4 Tesla magnetic field, with as compact a shower development as practical. The options considered include crystals, silicon-tungsten sampling, lead (or

	Requirement	Basis
EM calorimeter		
Energy resolution	$\sim 10\%/\sqrt{E} + 0.5\%$	$h \to \gamma\gamma$
Segmentation (transverse)		
towers	< 40 mrad	charged/neutral separation
μstrips at shower max	< 2 mrad	charged/neutral separation and electron identification
Spatial resolution	$\sim$0.3 mm at 100 GeV	charged/neutral separation
Timing	$\sim$ few nanoseconds	rejection of two-photon events
Charged hadron rejection	$< 1\%$	jet energy measurements
EM energy containment	depth = 30 X_0	energy resolution
Moliere radius	$\sim$7 mm	charge/neutral separation
Magnetic coil placement	outside EM calorimeter	EM energy resolution
Hadron calorimeter		
Jet resolution	$< 4\%$ at 100 GeV	Two-jet mass resolution
Depth	6 λ	Jet resolution
Angular coverage	$> 99\%$ 4π	Missing energy measurements
Segmentation	$\sim$ 40 mrad	neutral hadron energy measurements

Table I: Design goals for the NLC Calorimeter.

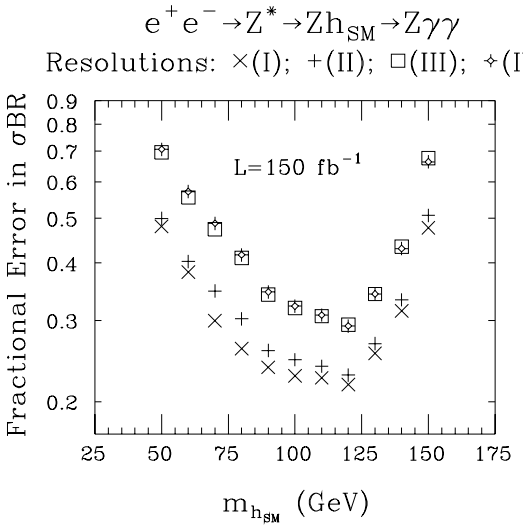

Figure 1: Fractional error in the measurement of $\sigma(Zh_{SM}) \cdot BR(h_{SM} \to \gamma\gamma)$ as a function of the Standard Model Higgs mass, assuming an integrated luminosity of 150 fb^{-1}. The four resolutions considered are (I) $2\% \oplus 0.5\% + 0.2\%/E$, (II) $5\%/\sqrt{E} \oplus 0.5\%$, (III) $10\%/\sqrt{E} \oplus 1\%$, and (IV) $12\%/\sqrt{E} \oplus 0.5\%$.[3]

tungsten) fiber, and scintillator sampling. We propose silicon-tungsten sampling for a variety of reasons. The silicon-tungsten technique can be deployed in a structure with excellent shower containment, based on a 7 millimeter radiation length and a Moliere radius of 20 millimeters. This can be done with a very high level of granularity, which is critical to the jet energy reconstruction described above in which charge and neutral energy must be separately measured. The energy resolution can be better than $14\%/\sqrt{E}$, depending on the sampling fraction, with a very small ($< 0.4\%$) constant term. Position resolution at the face of the calorimeter for electromagnetic showers would be $\sim$ 0.3 mm at 100 GeV, which translates to 0.6 mrad at 90°. Silicon has excellent energy response, such that timing of a few nanosecondes is conceivable. Other well-known advantages of silicon are its stable responses due to the linear charge collection and flexibility in choice of segmentation.

The main draw-back to the silicon-tungsten sampling option is its practical limit in electromagnetic resolution of about $10\%/\sqrt{(E)}$. We take the view that the other features, particularly the very high level of granularity ($\sim$ 4 million pads), justify the compromise on the resolution.

II. THE SILICON CALORIMETER OPTION

We propose a calorimeter with $30X_0$ of depth composed of tungsten plates with silicon sampling. The first 40 layers would be $0.5X_0$ thick sampling at normal incidence with the last $10X_0$ covered with $1X_0$ sampling. This configuration should yield a 12-14%/$\sqrt{E}$ electromagnetic energy resolution. Each layer would be transversly segmented into 1 cm^2 pads, and all 40 layers would be individually read out, as described below, resulting in a very finely segmented EM calorimeter. Two orthogonal layers of 1 mm pitch silicon microstrips would be deployed near shower maximum ($\sim 6X_0$) for shower position measurements.

The silicon-tungsten sampling calorimeter technique has been adopted with excellent success for luminosity monitoring at present-day e^+e^- colliders, first at SLD[5], and then at OPAL[6] and Aleph[7]. These experiments continue to run successfully more than 5 years after the first operation. The large scale silicon-tungsten calorimeter proposed here is a natural extension of these smaller systems.

Table II presents the list of the principle features of the EM calorimeter considered here.

A. Electronics

At the NLC trains of 90 bunches, with an interbunch spacing of approximately 1.4 ns, collide with repetion rate of 120 Hz to 180 Hz giving a spacing between trains of 5.5 to 8.3 ms. Because of the relatively low occupancy at the even the highest foreseen luminosity, it is not necessary for all elements of the detector to resolve individual bunches. Ideally the calorimeter electronics will provide both information about the amplitude

EM calorimeter	
Solid Angle Coverage	99.5% 4π
Segmentation	
Transverse	$.02\times.02$ at 90°
Longitudinal	$0.5X_0$
Total Depth	$30X_0$
Total Weight	23,768 kg
Barrel module	186 kg
Endcap (ea.)	1,468 kg
Number of Channels	4×10^6
per barrel module	20,000
Number of Modules	
Barrel	112
End Cap	64
Hadron calorimeter	
Solid Angle Coverage	99.5% 4π
Total Depth	6λ

Table II: Parameters of the Calorimeter. These parameters are chosen to achieve the Goals of Table I.

and time of the energy deposits in the calorimeter. The amplitude information can be averaged over all of the bunches in a train, and will be extremely detailed, giving separate pulse height for each silicon pad in the detector. The time information need not be as detailed. Longitudinal information will not be needed and the transverse granularity can be much larger than for the amplitude information.

One possibility for the electronics is similar to the AMPLEX approach[8] which has been successfully used in several silicon-tungsten calorimeters in the past. In this approach, each channel is equipped with a low noise preamplifier and a sample-and-hold unit, which is located close to the silicon detectors. After the train of bunches has past, all of the channels can then be read out using an analog multiplexing scheme. In our design, each layer of the calorimeter would be connected to a single analog output which would transport the multiplexed signals to digitizing electronics located at the back of each tower. With the present AMPLEX electronics, the analog signals are digitized at a rate of approximately 0.5 MHz. If each tower contains approximately 45,000 channels, approximately 25 ADC/tower would be needed to complete the digitization within 5 msec.

The AMPLEX approach also allows the outputs of the individual sample-and-holds units to be combined to form a "trigger" output. Although the "trigger" information is unlikely to be useful at the NLC where every channel could be digitized for each beam crossing, it is possible that the trigger information could be used for timing. A summed signal with a rise time of order ~ 1.5 ns is perhaps impossible, but it may be possible to identify the correct bunch with a much slower signal.

B. Mechanical Design

A possible mechanical design for the detector is shown in figure 2. This design divides the detector barrel into 112 towers. There are 16 divisions in azimuth and 7 in longitude. The gaps between modules are not projective and will be approximately 1 mm.

The stack of 50 tungsten plates will be held in place using

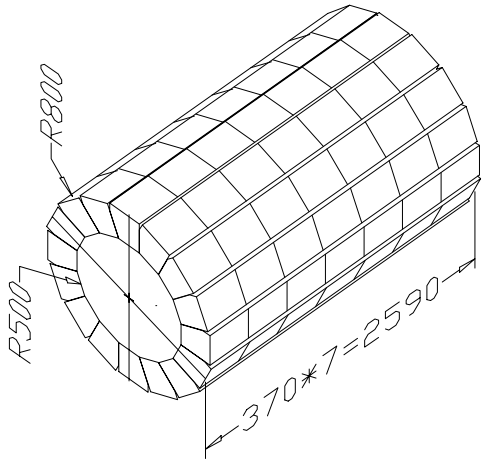

Figure 2: Possible mechanical layout for silicon-tungsten EM calorimeter barrel.

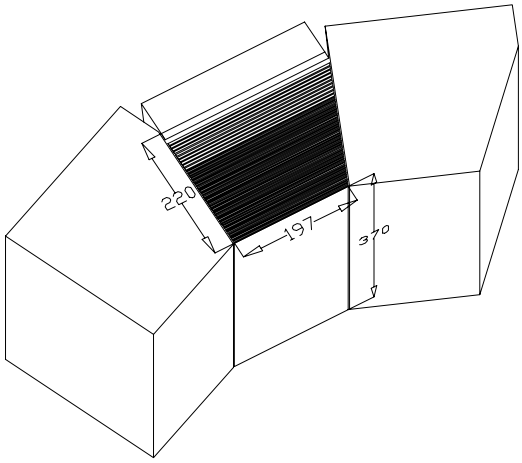

Figure 3: Possible mechanical layout for the EM module.

4 dowels of 3 mm diameter which penetrate each of the plates (see figure 3). In the air gaps, spacers around each dowel will be used to maintain the 1.8 mm clearance between layers. The layout of the silicon detectors will be varied from layer to layer so that a given shower will be unlikely to encounter the small cracks between detectors in successive layers of the calorimeter.

C. Cooling

A detailed cooling design of the detector has not yet been made. One possible approach is to employ air cooling. This minimizes dead space between towers and is possible if low power electronics ($\sim$ 50 μW/channel or less) can be used. A large reduction in the power consumption over electronics in use at storage rings can be realized, if the pre-amplifier and trigger portion of the electronics is powered only during the time the beams are actually colliding. At 180 Hz the NLC only has a duty cycle of 4.6×10^{-5}. This could reduce the power consumption of the pre-amplifier portion of the circuit to a negligible level. If care is taken in the design of the multiplexing stage of the front end electronics, it may be possible to meet or exceed the 50 μW goal.

The tungsten plates are separated from each other by 1.8 mm. Much of the space between layers will be needed for the silicon

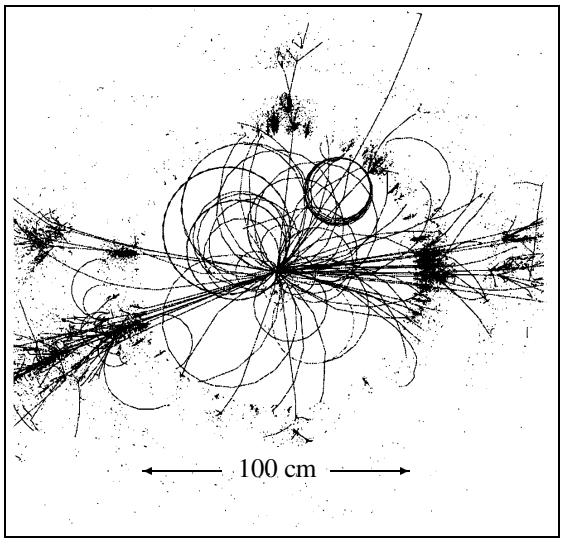

Figure 4: GEANT simulation of $e^+e^- \rightarrow Z^0h(120\ GeV)$ event. The inner region of this figure corresponds to the tracker and the inner surface of the electromagnetic calorimeter is evident from the onset of photon conversions[9].

detectors and the front electronics which will be mounted on thin kapton circuit boards. Gaps of 0.5 mm to 1.0 mm will remain for air cooling. Depending on the direction of the air flow (radial or longitudinal) flow rates between 10 cm/s and 50 cm/s would be needed.

III. JET RESOLUTION SIMULATION

Figure 4 presents a simulation of an event of the type $e^+e^- \rightarrow Z^0h(120\ GeV)$ interacting in the NLC EM calorimeter described above[9]. In order to clearly display the energy deposition, the structure of the detector is not shown. This projection of the detector covers about 1 m × 1 m. The inner surface of the EM calorimeter, at a radius of 50 cm, is clearly seen where the photons are converted to EM showers. This image give a qualitative feel for the ability of a high granularity EM calorimeter to separate the neutral electromagnetic clusters.

The fluctuations in neutrino energy in jets contribute an irreducible limit on the resolution of energy measurement, although event constraints can partially ameliorate these fluctuations. The jet measurement technique being proposed here seeks to build from the excellent tracking measurements, with the measurement of neutral particles (gammas, neutrons, K^0_Ls, etc.) in the calorimeter. Table III shows the contribution of the non-EM neutral components of events to the rms fluctuation of observed total energy for events of the type $e^+e^- \rightarrow Z^0h(120\ GeV)$, $Z^0(\rightarrow q\overline{q})$, $(h_{120\ GeV} \rightarrow b\overline{b})$. The jet resolution of the detector is ultimately limited by the fluctuations in neutrino energy, which exceed 5% for the Higgs events.

Figure 5 shows the gamma-charged hadron separation at the calorimeter. For gammas from $e^+e^- \rightarrow Z^0h(120\ GeV)$ of more than 10 GeV, the distance at the calorimeter face to the entrance point of the closest charged hadron of at least 10% of the gamma energy is plotted. It is necessary to separate the gammas from the charged tracks within a few millimeters.

	average observed energy	rms of observed energy	resolution
No ν	480 GeV	25 GeV	5.3%
No ν or n	460 GeV	34 GeV	7.3%
No ν, n, or K^0_L	434 GeV	39 GeV	9.0%

Table III: Energy Resolution for Total Event Energy.

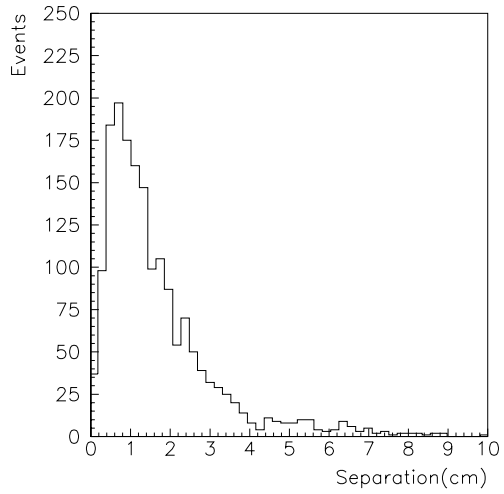

Figure 5: Separation (in centimeters) between gammas and the closest charged track at the calorimeter face for gammas with more than 10 GeV of energy and charged tracks with at least 10% of the gamma energy.

We assume, conservatively, that the highly segmented calorimeter described above will begin failing to separate EM showers and charged tracks when they strike the calorimeter within 1.4 cm. We assume the neutral EM showers within 1.4 cm of a charged hadron at the calorimeter face are measured with the usual EM resolution of $12\%/\sqrt{E} \oplus 1\%$, 93% of the time, with the remaining 7% of the showers lost. For other neutral showers and charged tracks the reconstruction efficiency is conservatively assumed to be 98%. The resolution on neutral hadrons is assumed to be $45\%/\sqrt{E} \oplus 2\%$. Directional smearing is imposed on all reconstructions. Under these assumptions, we expect the two-jet mass distribution for a 120 GeV higgs boson in the reaction shown in figure 6.

The mass resolution in figure 6 of 8 GeV/c^2 is dominated by the loss of energy from neutrinos. Here energy and momentum balance have been imposed on the four jets in each event after events with more than 10 GeV of missing transverse energy have been removed to reduce the effect of neutrinos. This results in a loss of just over 50% of the events. A more detailed fit to the events could improve the resolution.

IV. BACKGROUNDS

The major backgrounds that must be considered for the calorimeter are synchrotron radiation, lost particles, the muon halo, and mini-jets which are enhanced by the beamstrahlung.

The synchrotron radiation backgrounds have been extensively

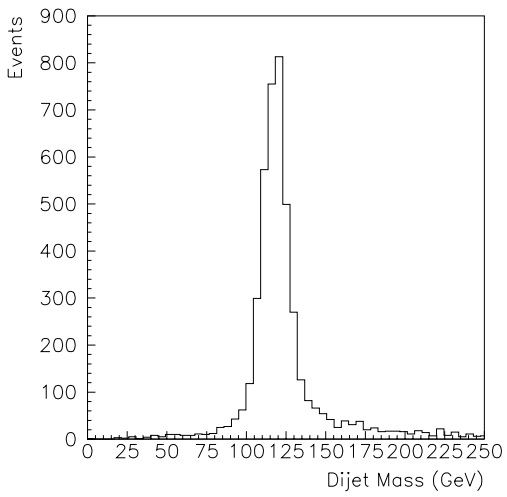

Figure 6: Two-jet mass distribution (in Gev/c^2) for the jet pair identified as h in $e^+e^- \rightarrow Z^0h(120\ GeV)$ events. A gaussian fit to the peak gives a sigma of about 8 GeV/c^2. See text for description of jet reconstruction.

studied and are being handled with masks and apertures following the experience with SLC/SLD[10]. The muon halo will be reduced to less than 1 muon per beam crossing with magnetized iron muon spoilers in the tunnel upstream of the final focus. The lost particles are handled by shielding.

Mini-jets pose a potentially large background, but are restricted to low transverse energy. Typically they fall off with $p_t^{-4.7}$ and are directed into the endcaps[11]. At $\sqrt{s} = 500$ GeV one expects a few percent per bunch crossing with $p_T > 2.5$ GeV. By tagging calorimeter events at the bunch-crossing time, this background becomes small, and increasing the p_T requirement is available to further suppress the signals.

V. RESEARCH AND DEVELOPMENT

Further research is needed on number of points to validate this approach to calorimetry for a compact detector at a future linear collider.

Detailed Monte Carlo studies are needed to develop pattern recognition software which can make full use of the transverse and longitudinal granularity of the detector to separate photons from charged particles. Similar studies will be needed to determine the granularity needed in the hadron section of the calorimeter for identification of neutral hadrons.

Monte Carlo studies will also be needed to optimize the energy resolution of the device. Present plans call for 40 half-radiation-length samples followed by 10 one-radiation-length samples; however, another sampling choice may produce a better overall resolution. These Monte Carlo studies must be validated either by using existing test beam data, or in the case of novel sampling techniques, by testing prototype calorimeters.

The biggest technical challenge for the construction of the calorimeter will be the development of electronics within the power requirements imposed by air cooling. Work should be done on both sides of the equation. Cooling design work is needed to optimize the configuration of the air flow. Once the optimized cooling design is in place, it can be tested using a prototype module with dummy heat loads. Similarly, significant electronics development is needed to adapt high density multiplexing schemes to the unique environment of a linear collider.

Futher work is also needed to optimize the overall mechanical design of the calorimeter so as to minimize the dead space between modules and at the same time allow for a practical cooling design.

Final validation of this calorimeter concept will require that prototype electronics and a prototype mechanical design be subjected to a beam test to show that the desired spatial and energy resolution can be achieved.

VI. CONCLUSIONS

We have examined the option of a high granularity silicon-tungsten sampling electromagnetic calorimeter combined with a relatively well segmented hadron calorimeter for the NLC Detector. The requirements and constraints on the NLC Calorimeter appear to be well satisfied by this approach. This technique provides enormous strength in understanding the details of jet energy deposition, and therefore, can provide excellent jet energy resolution.

∗ This research was supported by the U.S. Department of Energy grant DE-FG03-96ER40969.

VII. REFERENCES

[1] V. Barger *et al.* "Probing Strongly Interacting Electroweak Dynamics Through W^+W^-/ZZ Ratios at Future e^+e^- Colliders," Phys Rev D52, 3815, 1995.

[2] P. Janot, "Higgs Boson Search at a 500 GeV e^+e^- Collider," Workshop on Physics and Experiments with Linear e^+e^- Colliders, Waikoloa, Hawaii, April, 1993.

[3] J. Gunion and P. Martin, "Prospects for and Implications of Measuring the Higgs to Photon-Photon Branching Ratio at the Next Linear e^+e^- Collider," proceedings of this Workshop.

[4] C.J.S. Damerell, "Ideas for the NLC Detector," proceedings of this Workshop.

[5] S.C. Berridge *et al.*, "First Results from the SLD Silicon Calorimeters," IEEE Trans. Nucl. Sci 39, 1242, (1992).

[6] B.E. Anderson *et al.*, "The OPAL Silicon-tungsten Calorimeter Front-End Electronics" IEEE Transactions on Nuclear Science Vol. 41, No. 4, Aug. 1994, 845-852.

[7] D. Bederede, *et al.*, "SICAL: A high precision silicon-tungsten luminosity calorimeter for ALEPH', NIM A365:117-134,1995.

[8] E. Beuville, et al., *Nucl. Inst. Meth.* **A288** (1990)157.

[9] Basem Barakat, private communication.

[10] S.S. Hertzbach, T.W. Markiewicz, T. Maruyama and R. Messner, "Backgrounds at the Next Linear Collider," proceedings of this workshop.

[11] T. Tauchi and H. Hayashii, "Inclusive Jet Measurements in $\gamma\gamma$ Collisions at Tristan and Estimation of Minijets for Future Linear Colliders," Workshop on Physics and Experiments with Linear e^+e^- Colliders, Waikoloa, Hawaii, April, 1993.